



Optics Letters

Optical pulse interharmonic extraction and repetition rate division based on a microwave photonic phase detector

KUNLIN SHAO,¹ PING LI,¹ YAMEI ZHANG,^{1,*} SHAOBO LI,² XIAODONG LIANG,² ANNI LIU,² AND SHILONG PAN^{1,3} 

¹Key Laboratory of Radar Imaging and Microwave Photonics, Ministry of Education, Nanjing University of Aeronautics and Astronautics, Nanjing 210016, China

²The 54th Research Institute of China Electronics Technology Group Corporation, Shijiazhuang 050081, China

³pans@nuaa.edu.cn

*zhang_ym@nuaa.edu.cn

Received 31 January 2023; revised 17 March 2023; accepted 18 March 2023; posted 20 March 2023; published 7 April 2023

Microwave photonic phase detectors (MPPDs) can extract ultrastable microwaves from a mode-locked laser (MLL), but their frequencies are often limited by the pulse repetition rate. Few works studied methods to break the frequency limitation. Here, a setup based on an MPPD and an optical switch is proposed to synchronize an RF signal from a voltage-controlled oscillator (VCO) to an interharmonic of an MLL and to realize the pulse repetition rate division. The optical switch is employed to realize pulse repetition rate division, and the MPPD is followed to detect the phase difference between the frequency-divided optical pulse and the microwave signal from the VCO, which is then fed back to the VCO via a proportional–integral (PI) controller. Both the optical switch and the MPPD are driven by the signal from the VCO. When the system reaches its steady state, the synchronization and repetition rate division are achieved simultaneously. An experiment is conducted to verify the feasibility. The 80¹/₂th, 80¹/₃rd, and 80²/₃rd interharmonics are extracted, and pulse repetition rate division factors of two and three are realized. The phase noises at offset frequency of 10 kHz are improved by more than 20 dB. © 2023 Optica Publishing Group

<https://doi.org/10.1364/OL.486694>

The characteristics of ultralow timing jitter and ultrahigh phase coherence make a mode-locked laser (MLL) an outstanding source for ultrastable microwave signal generation [1,2], which is highly desirable in radar, communication, and measurement systems [3–5], etc. During the last decade, substantial studies focused on extracting a microwave signal with a low phase noise from an MLL, which can be generally categorized into two types. The approaches in the first category are directly beating the output of an MLL by a photodetector (PD) [6–9], and this structure can obtain a series of microwave frequency components. With a sophisticated setup, such as locking the MLL to an ultrastable laser source or multiplying the repetition rate of the MLL with a Mach–Zehnder interferometer (MZI), a microwave signal with an ultralow phase noise can be generated [7,8]. The

second category is using a microwave photonic phase detector (MPPD) [10–16] to lock an external voltage-controlled oscillator (VCO) to one harmonic of the pulse repetition rate of the MLL. By detecting the phase error between the optical pulse train and the microwave signal from the VCO with the MPPD, and feeding the phase error back to the VCO, the VCO can be locked to the MLL. Based on this method, a wideband tuned microwave signal [14] and a two-tone microwave signal [15] with an ultralow phase noise have been produced recently. However, in most MLL-based microwave signal extraction systems, the frequency of the microwave signal is limited to N times the pulse repetition rate (where N is an integer). To acquire other frequencies from the MLL, one direct way is to adjust the laser cavity length. However, sophisticated schemes are required to stabilize the cavity. Optical switches might also help generate new frequency components since they can select one pulse from every N pulses to realize $1/N$ frequency division. However, an external RF source and a synchronization clock with a specific frequency are required, making the system complicated [17,18]. Recently, interharmonic extraction from an MLL was realized via an MPPD [19], providing a new way to generate microwave frequencies of non-integer multiples of the pulse repetition rate. The approach applies high driven power to stimulate nonlinearity, and the bias of the MPPD needs adjustment for different frequencies.

In this Letter, a system for simultaneous interharmonic extraction and optical pulse repetition rate division is proposed and demonstrated, for the first time to our best knowledge, using a Mach–Zehnder modulator (MZM) based optical switch [20] and a dual-polarization dual-drive MZM (DP-DMZM) based MPPD. Both the optical switch and the MPPD are driven by a microwave signal from a VCO. An optical pulse train from an MLL turns into a frequency-divided optical pulse after passing through the optical switch. The MPPD helps discriminate the phase difference between the microwave signal and the frequency-divided optical pulse train. The phase difference is then fed back to the VCO via a proportional–integral (PI) controller. When the system reaches a steady state, the repetition rate division is achieved at the output of the MZM, and the VCO

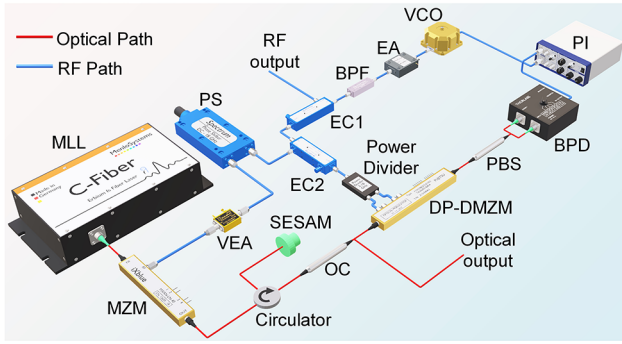


Fig. 1. Structure of proposed system. BPD, balanced photodetector; BPF, bandpass filter; DP-DMZM, dual-polarization dual-drive MZM; EA, electrical amplifier; EC, electrical coupler; MLL, mode-locked laser; MZM, Mach-Zehnder modulator; OC, optical coupler; PBS, polarization beam splitter; PI, proportional-integral controller; PS, phase shifter; SESAM, semiconductor saturable absorber mirror; VCO, voltage-controlled oscillator; VEA, variable electrical attenuator.

is locked to an interharmonic of the repetition rate. MLLs with arbitrary repetition rates can be frequency divided based on this structure.

The proposed interharmonic extraction and repetition rate division system is illustrated schematically in Fig. 1, and consists of an MLL, an MZM, a circulator, a semiconductor saturable absorber mirror (SESAM), an optical coupler, a DP-DMZM, a polarization beam splitter (PBS), a balanced PD (BPD), a PI controller, a VCO, an electrical amplifier, a bandpass filter, two RF couplers, an RF power divider, a phase shifter, and a variable electrical attenuator. To show the principle in an explicit way, we assume the system has reached a steady state. Supposing that the optical pulse train from the MLL is expressed as

$$E_{\text{pulse}}(t) = \sqrt{P} \sum_{n=0}^{\infty} \delta(t - nT_{\text{rep}}), \quad (1)$$

where P is the peak power of each pulse, and T_{rep} is the minimum positive period of the optical pulse train. The microwave signal from the VCO is written as

$$m(t) = A \sin(2\pi(N + q)f_{\text{rep}}t + \varphi) \quad (q = 1/2, 1/3, 2/3), \quad (2)$$

where A and φ are the amplitude and phase of the microwave signal, respectively, and N is an integer. Equation (2) indicates that the frequency of the microwave signal equals the interharmonic of the original pulse repetition rate.

The optical pulse train is first sent into the MZM, which is driven by part of the microwave signal from the VCO. The transfer function of the MZM is

$$h(t) = \cos\left(\frac{\pi a}{V_{\pi}} \cos(2\pi(N + q)f_{\text{rep}}t) + \theta\right), \quad (3)$$

where a is the microwave signal amplitude, and V_{π} and θ are the half-wave voltage and DC-bias phase of the MZM, respectively. Thus, the pulse at the output of the MZM is given by

$$E(t) = E_{\text{pulse}}(t) \cdot h(t) = \sqrt{P} \sum_{n=0}^{\infty} \cos\left(\frac{\pi a}{V_{\pi}} \cos(2\pi nq) + \theta\right) \delta(t - nT_{\text{rep}}). \quad (4)$$

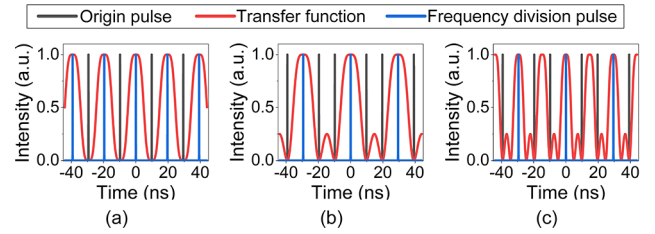


Fig. 2. Transfer function of MZM-based optical switch and optical pulse before and after MZM with (a) 51-MHz driven signal, (b) 34-MHz driven signal, and (c) 68-MHz driven signal.

From Eq. (4), when a and θ are set at appropriate values, the repetition rate of the optical pulse varies. In the following, we take the case when q equals $1/3$ as an example.

Since q equals $1/3$, the period of the pulse train changes to $3T_{\text{rep}}$. Therefore, only n equals 0, 1, 2 should be taken into consideration. Assuming that the pulse amplitude maintains itself when $n = 0$, and vanishes when $n = 1, 2$, an equation set is obtained:

$$\begin{cases} \cos\left(\frac{\pi a}{V_{\pi}} + \theta\right) = 1 \\ \cos\left(-\frac{\pi a}{2V_{\pi}} + \theta\right) = 0 \end{cases}. \quad (5)$$

One of the solutions is

$$a = \frac{V_{\pi}}{3}, \quad \theta = -\frac{\pi}{3}. \quad (6)$$

Thus, Eq. (4) changes to

$$E(t) = \sqrt{P} \sum_{k=0}^{\infty} \delta(t - 3kT_{\text{rep}}). \quad (7)$$

It should be noted that the repetition rate of the optical pulse is divided by three. For q equals $2/3$, it is the same as the case that q equals $1/3$. For q equals $1/2$, similar to this process, different values of a and θ are required:

$$a = \frac{V_{\pi}}{4}, \quad \theta = -\frac{\pi}{4}. \quad (8)$$

In other words, by adjusting the amplitude of the driven power and the bias point of the MZM, different repetition rate division factors can be obtained. Figure 2 gives the simulation results of the repetition rate division process. The pulse repetition rate is set as 102 MHz, and the frequencies of the microwave signals driving the MZM are set as 51 MHz, 34 MHz, and 68 MHz, respectively, which are equivalent to $51 \text{ MHz} + Nf_{\text{rep}}$, $34 \text{ MHz} + Nf_{\text{rep}}$, and $68 \text{ MHz} + Nf_{\text{rep}}$. The black lines represent the original optical pulse train, the red lines represent the transfer functions of the MZM, and the blue lines are the frequency-divided optical pulse trains at the output of the MZM. Figure 2(a) shows the case with 51-MHz microwaves, and the repetition rate division factor of two at the output of the MZM is realized. Figures 2(b) and 2(c) show the cases with 34-MHz and 68-MHz microwaves, and both repetition rate division factors of three are achieved.

The frequency-divided optical pulse train then transmits through a SESAM to further suppress the unwanted pulse components in the time domain. Then, the pulse train is injected into a DP-DMZM based MPPD. The principle of the MPPD was previously detailed by Shao *et al.* [13]. When a microwave

signal from the VCO is applied to the DP-DMZM, the output of the DP-DMZM would be denoted as

$$\begin{bmatrix} E_x \\ E_y \end{bmatrix} \propto \begin{bmatrix} \cos\left(\beta \sin \varphi + \frac{\pi}{4}\right) \\ \cos\left(\beta \sin \varphi - \frac{\pi}{4}\right) \end{bmatrix} \sum_n \delta(t - nT_{\text{rep}}), \quad (9)$$

where β is the modulation index, $n = 2k$ when $q = 1/2$, and $n = 3k$ when $q = 1/3$ or $2/3$ (k is an integer). A PBS is followed to split the two orthogonal polarization signals. A low-speed BPD is utilized to detect the average power difference between the two orthogonal polarization signals. The output of the BPD is

$$\Delta P \propto G\mathfrak{R} \sin(2\beta \sin \varphi) \approx 2G\mathfrak{R}\beta\varphi, \quad (10)$$

where G is the trans-impedance gain of the BPD, and \mathfrak{R} is the responsivity of the BPD. From Eq. (10), the phase difference between the optical pulse and the microwave is detected successfully, and thus the VCO can be locked to the MLL.

An experiment is conducted based on the setup characterized in Fig. 1 to verify the validity of the system. An MLL (Menlo, C-Fiber) is exploited to emit an original optical pulse train with a repetition rate of 100.4 MHz, which is launched to an MZM (iXblue, MXAN-LN-40) based optical switch. The MZM has a half-wave voltage of around 5.5 V and an extinction ratio of around 17 dB. A VCO (HMC-C200 8050) with a frequency tuned from 8.05 GHz to 8.13 GHz is employed to produce the 80^{1/2}th (8.082 GHz), 80^{1/3}rd (8.065 GHz), and 80^{2/3}rd (8.099 GHz) interharmonics. After being amplified and filtered, the VCO output is split into three paths. One is applied to the MZM, one is applied to an MPPD, and the third is monitored by a signal analyzer. After the optical switch, the optical pulse would be frequency divided, and is then injected into the MPPD, which is configured by a DP-DMZM (Fujitsu, FTM 7980), a PBS, and a BPD (THORLABS, PDB450C). The phase information from the BPD is processed by a PI controller (New Focus, LB1005) before being fed back to the VCO. When the system reaches a steady state, the output from the VCO will be synchronized to an interharmonic of the MLL.

Figure 3 presents the spectra of the locked microwave signals, the 80th and the 81st MLL harmonics. In Fig. 3(a), microwave signals located at 1/3, 1/2, and 2/3 positions between two MLL harmonics are observed. Figures 3(b), 3(c), and 3(d) are expanded versions of the microwave signals. The resonant peaks are caused by the transfer function of the closed phase locked loop.

The waveform envelope of the optical output signal and its spectrum are captured by a 50-GSa/s oscilloscope (Tektronix, DSA72004B) and a spectrum analyzer, respectively, after being detected by a high-power PD (Finisar, VPDV2120-VF-FA), and are depicted in Fig. 4. In Figs. 4(a), 4(c) and 4(e), the black curves represent the original pulse envelopes from the MLL, and the other curves represent the frequency-divided pulses at the optical output of the system. In Figs. 4(b), 4(d), and 4(f), the black curves are the spectra from the MLL, and the other curves represent the spectra at the optical output of the system. When the VCO emits a signal with a frequency of 8.082 GHz, the pulse period doubles and the repetition rate is divided by two. When the VCO emits a signal with a frequency of 8.065 GHz or 8.099 GHz, both the pulse periods triple, and repetition rates division factors of three are achieved.

To verify the interharmonic locking performance, the phase noises of the microwave signals are measured by a phase

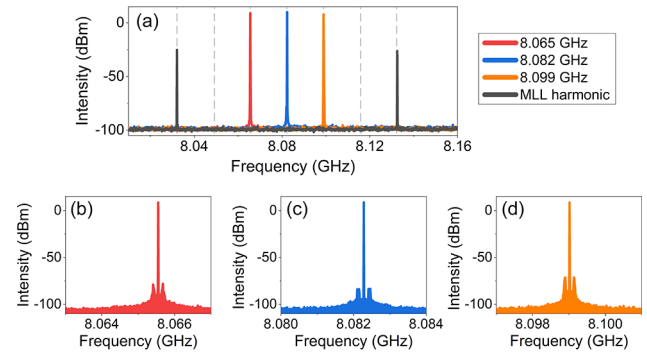


Fig. 3. (a) Spectra of MLL harmonic and locked microwaves. (b) to (d) Enlarged (b) 8.065-GHz signal spectrum, (c) 8.082-GHz signal spectrum, and (d) 8.099-GHz signal spectrum.

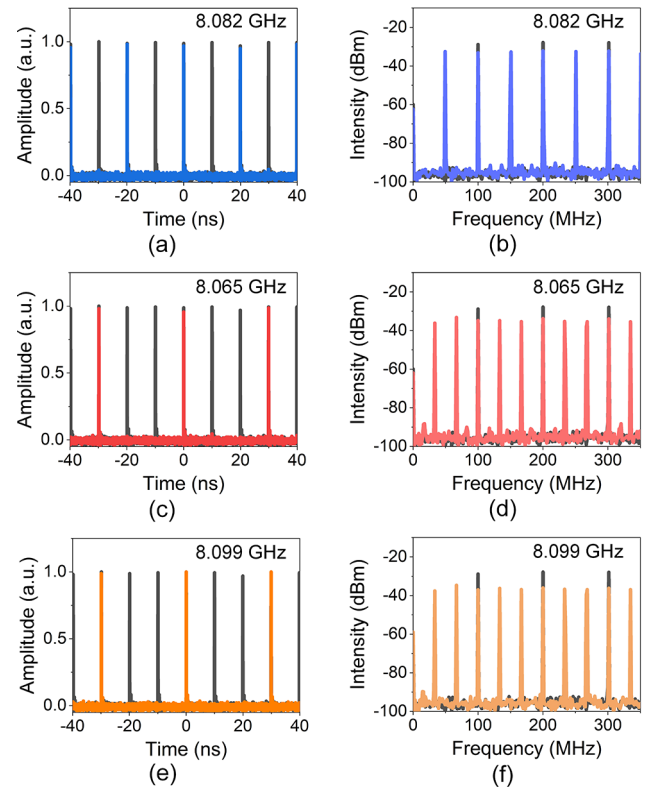


Fig. 4. (a) Waveform and (b) spectrum of optical pulse when 8.082-GHz signal is locked. (c) Waveform and (d) spectrum of optical pulse when 8.065-GHz signal is locked. (e) Waveform and (f) spectrum of optical pulse when 8.099-GHz signal is locked.

noise analyzer (Rode & Schwarz, FSWP50), as displayed in Fig. 5. The phase noises of the 8.082-GHz, 8.065-GHz, and 8.099-GHz signals are, respectively, shown in Figs. 5(a), 5(c), and 5(e). In each figure, the dashed pink curve is the phase noise of the free-running VCO, and the gray curve (closed squares) is the phase noise of the 80th harmonic of the MLL. The solid curves without symbols are the phase noises of the locked microwaves. The phase noises of the locked signals and the 80th MLL harmonic are approximate. This is because the three microwave frequencies are adjacent to that of the 80th MLL harmonic, and the difference between their phase noises is imperceptible. Compared with the

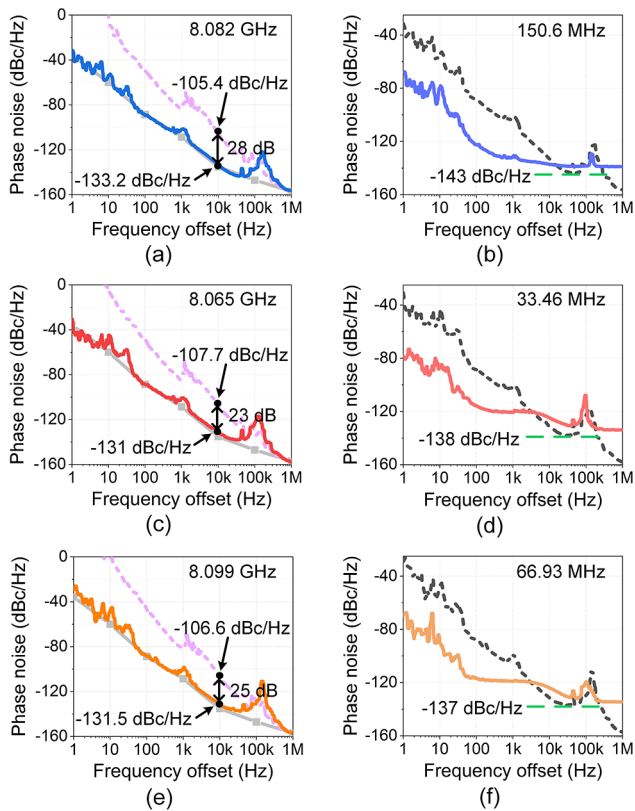


Fig. 5. (a), (c), and (e) Phase noises of (a) 8.082-GHz signal, (c) 8.065-GHz signal, and (e) 8.099-GHz signal. (b), (d), and (f) Phase noises of the downconversion signals with frequencies of (b) 150.6 MHz, (d) 33.46 MHz, and (f) 66.93 MHz. Gray curves are the phase noise of the 80th harmonic of the MLL. Dashed black curves are the phase noises of the locked interharmonic signals.

free-running VCO, the phase noise of the locked VCO improves dramatically. At 10-kHz offset frequency, the phase noise reduces from -105.4 dBc/Hz (-107.7 dBc/Hz, -106.6 dBc/Hz) to -133.2 dBc/Hz (-131.0 dBc/Hz, -131.5 dBc/Hz) for microwaves with a frequency of 8.082 GHz (8.064 GHz, 8.099 GHz). More than 20 dB improvement is achieved. The figures also indicate that the noise floor of the MPPD is around -140 dBc/Hz.

To evaluate the coherence between the locked microwave and the original optical pulse qualitatively, an electrical mixer is used to mix the locked microwave with an MLL harmonic. It is known that if two signals with different frequencies are coherent, the phase noise of their downconverted signal will be smaller than that of the signal with higher frequency; thus the phase noise in the locking bandwidth should reduce after the VCO output mixed with the MLL harmonic. Part of the original optical pulse is injected into a PD to get the MLL harmonic. The phase noise analyzer we use shows a malfunction in measuring a 50-MHz signal phase noise accurately, while signals with other frequencies are not affected; therefore, the 8.082-GHz signal is mixed with the 79th harmonic to produce a 150.6-MHz downconverted signal. The 8.064-GHz and 8.099-GHz signals are mixed with the 80th harmonic of the MLL, and downconverted signals with frequencies of 33.46 MHz and 66.93 MHz are obtained. The phase noises of the three downconverted signals are plotted in Figs. 5(b), 5(d), and 5(f) (solid curves), respectively. The dashed

black curve in each figure is the phase noise of the corresponding microwave after being locked to the interharmonic. It is observed that the phase noises of the downconverted signals at low offset frequencies are much smaller than those of the locked microwaves (dashed black curves); this indicates that the locked microwave and the optical pulse train show good coherence. The phase noises of downconverted signals at high offset frequencies are limited by the mixing efficiency and the noise floor of the MPPD. However, the long-term stability of the system is not that good, owing to the bias drift of the MZM. We believe that the long-term stability can get an improvement by replacing the MZM with a Sagnac loop interferometer consisting of a passive nonreciprocal optical phase shifter as in Jung and Kim [10].

In summary, we have demonstrated a versatile system to realize optical pulse interharmonic extraction and repetition rate division jointly for the first time to the best of our knowledge. The system extracts the 80^{1/2}th, 80^{1/3}rd, and 80^{2/3}rd interharmonics of the MLL successfully. They all show good coherence with the pulse from the MLL, and the phase noises at 10-kHz offset frequency are improved by more than 20 dB. Meanwhile, the pulse repetition is divided by two and three.

Funding. National Natural Science Foundation of China (61901215, 62271249).

Disclosures. The authors declare no conflicts of interest.

Data availability. Data underlying the results presented in this paper are not publicly available at this time but may be obtained from the authors upon reasonable request.

REFERENCES

- J. Kim and Y. Song, *Adv. Opt. Photonics* **8**, 465 (2016).
- N. Kuse, J. Jiang, C.-C. Lee, T. Schibli, and M. Fermann, *Opt. Express* **24**, 3095 (2016).
- S. Pan and Y. Zhang, *J. Lightwave Technol.* **38**, 5450 (2020).
- E. A. Kittlaus, D. Eliyahu, S. Ganji, S. Williams, A. B. Matsko, K. B. Cooper, and S. Forouhar, *Nat. Commun.* **12**, 4397 (2021).
- Y. Na, C.-G. Jeon, C. Ahn, M. Hyun, D. Kwon, J. Shin, and J. Kim, *Nat. Photonics* **14**, 355 (2020).
- T. M. Fortier, M. S. Kirchner, F. Quinlan, J. Taylor, J. C. Bergquist, T. Rosenband, N. Lemke, A. Ludlow, Y. Jiang, C. W. Oates, and S. A. Diddams, *Nat. Photonics* **5**, 425 (2011).
- A. Haboucha, W. Zhang, T. Li, M. Lours, A. N. Luiten, Y. Le Coq, and G. Santarelli, *Opt. Lett.* **36**, 3654 (2011).
- X. Xie, R. Bouchand, D. Nicolodi, M. Giunta, W. Hänsel, M. Lezius, A. Joshi, S. Datta, C. Alexandre, M. Lours, P.-A. Tremblin, G. Santarelli, R. Holzwarth, and Y. Le Coq, *Nat. Photonics* **11**, 44 (2017).
- M. Hyun, C.-G. Jeon, and J. Kim, *Sci. Rep.* **11**, 17809 (2021).
- K. Jung and J. Kim, *Opt. Lett.* **37**, 2958 (2012).
- C.-G. Jeon, Y. Na, B.-W. Lee, and J. Kim, *Opt. Lett.* **43**, 3997 (2018).
- J. Wei, S. Zhang, J. Kim, and S. Pan, *J. Lightwave Technol.* **36**, 4267 (2018).
- K. Shao, S. Liu, P. Gao, Y. Zhang, Z. Y. Xu, H. Wang, and S. L. Pan, *IEEE Photonics Technol. Lett.* **35**, 385 (2023).
- M. Bahmanian and J. C. Scheytt, *IEEE Trans. Microwave Theory Tech.* **69**, 1635 (2021).
- K. Shao, Y. Zhang, P. Gao, F. Yang, J. Zhao, S. Liu, P. Li, X. Tang, Z. Xu, and S. Pan, *J. Lightwave Technol.* **41**, 637 (2023).
- C. Ahn, Y. Na, M. Hyun, J. Bae, and J. Kim, *Photonics Res.* **10**, 365 (2022).
- T. S. Khwaja and T. H. Yoon, *Phys. Rev. A* **102**, 043515 (2020).
- H. Ye, L. Pontagnier, C. Dixneuf, G. Santarelli, and E. Cormier, *Opt. Express* **28**, 37209 (2020).
- M. Bahmanian, C. Kress, and J. C. Scheytt, *Opt. Express* **30**, 7763 (2022).
- Y. Zhang, C. Liu, K. Shao, Z. Li, and S. Pan, *Opt. Lett.* **45**, 2038 (2020).